Supplementary information

Receptor Design and Extraction of Inorganic Fluoride Ion from Aqueous Solution

Priyadip Das, Amal K. Mandal, Manoj K. Kesharwani, E. Suresh, Bishwajit Ganguly* and

Amitava Das*

Central Salt and Marine Chemicals Research Institute (CSIR),

G.B. Marg, Bhavnagar: 364002, Gujarat, India.

Email address: ganguly@csmcri.org, amitava@csmcri.org

Telephone number: +91 278 2567760 [672]; Fax number: +91 278 2567562/6970

Table of Contents:-

Materials and method:

The chemical such as 2,3 dimethyl anthraquinone, N-bromo succinamide (NBS) dibenzoyl peroxide , trtrabutyl ammonium salt of various anions and sodium hexafluoro phosphate were obtained from sigma-Aldrich and were as received without any purification, Triphenyl phosphene, sodium fluoride and all the other reagents used were of reagent grade (S. D. Fine chemical, India) and were used as received.Various analytical and spectroscopic data obtained for these intermediates provided necessary supports for the proposed formulation and required purity. HPLC grade acetonitrile (Fisher Scientific), water was used as a solvent. Chloroform, Methanol, carbon tetrachloride was used for different synthetic procedure and studies, were purified through distillation following standard procedures, prior to use. Microanalysis (C, H, N) were performed using a Perkin-Elmer 4100 elemental analyzer. FTIR spectra were recorded as KBr pellets using Perkin Elmer Spectra GX 2000 spectrometer. ^1H and ^{31}P NMR spectra were recorded on Bruker 200 MHz (Avance-DPX 200)/ 500 MHz (Bruker Avance II 500) FT NMR. Electronic spectra were recorded with Cary-Varian UV-VIS NIR spectrophotometer

Synthetic scheame:

3
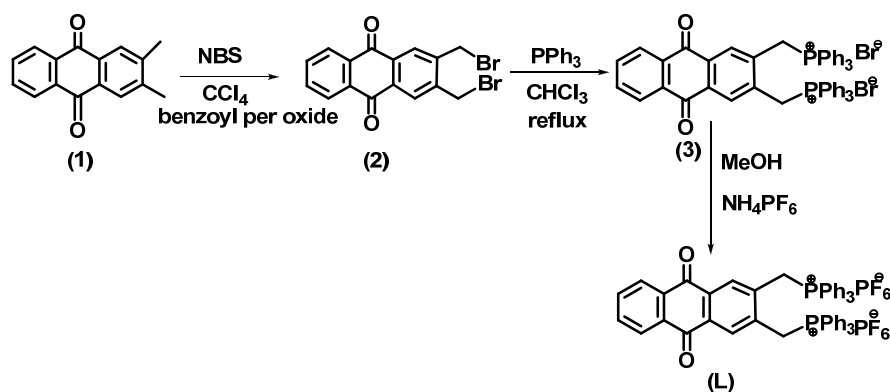
Synthesis of 2 (2,3 dimethyl bromo anthraquinone):

N-bromosuccinamide (NBS) (662.2 mg, 3.7243 mmol) and a catalytic amount of recrystallized dibenzoylperoxide were added to a solution of **1** (400mg, 1.6929mmol dissolved in 80 ml of CCl_4). The resulting mixture was refluxed for 4 h with irradiation of a100 W lamp. The decomposed product of NBS was then separated by filtration and the filtrate was evaporated to dryness to afford a yellow coloured solid residue, which was subjected to column chromatography on silica gel as stationary phase and chloroform/hexane solvent mixture (1:1, v/v) as the eluent to get the **2** as a pure product (480 mg, 71.2%). ^{1}H NMR (200 MHz, $CDCl_3$, 25 °C, TMS) δ (ppm): 8.348 - 8.33 (m, 2H; ArH), 8.30 (s, 2H; ArH), 7.87 – 7.812(m, 2H; ArH), 4.760(s, 4H; -CH_2). IR (KBr) ν_{max}/cm^{-1}: 3037, 1677, 1589, 1331, 1298, 1227, 966, 795, 714, 622. ESI-MS (m/z): 415 (($M^+ + Na^+$), 100%). Elemental analysis: $C_{16}H_{10}Br_2O_2$: calculated C (48.77), H (2.56); found C (48.21), H (2.73).

Synthesis of 3 (2,3-Bis(triphenylposphoniomethyl)anthraquinone dibromide):

A solution of **2** (200mg, 0.508mmol) and triphenyl phosphene (281mg, 1.117mmol) in 50ml dry chloroform was refluxed for 3-4 hrs , then the reaction mixture was allowed to stir at room temperature for 14 hrs. Then the reaction mixture was evaporated to dryness to afford a thick oily residue, this was treated with diethyl ether and on constant stirring afford a yellowish solid residue, which was filtered off, dried properly and finally recrystalised from minimum volume of chloroform to get the pure product **3** (428mg, 92%). ^{1}H NMR (500 MHz, $CDCl_3$, 25 °C, TMS) δ (ppm): 8.208-8.198 (m, 6H; ArH), 7.827 (s, 2H; ArH), 7.692 – 7.653 (m, 20H; ArH), 7.556 (t, J = 7Hz, 2H; ArH), 7.488 – 7.473 (m, 6H; ArH), 6.785 (d, J = 15.5Hz, 4H; Ar-CH_2P), . IR (KBr) ν_{max}/cm^{-1}: 3462, 3056, 1674, 1589, 1436, 1328, 1298,1111, 718, 690, 539, ESI-MS (m/z): 839 ((M^+ - Br^-), 20%), 757.28 ((M^+ - $2Br^-$), 30%). Elemental analysis: $C_{52}H_{40}O_2P_2Br_2$: calculated C (67.99), H (4.39); found C (66.85), H (4.51).

**Synthesis of L (2, 3-Bis(triphenylphosphoniomethyl)anthraqunone di hexa fluorophosphates:**

To a solution 0.1g (0.476mmol) of 2, 3-bis(triphenylphosphoniomethyl)anthraquinone dibromide (**3**) in 20mL of MeOH, $NaPF_6$ (0.106g, 0.654 mmol) was added. The reaction mixture was stirred for 5hrs, which afford a yellow precipitate. The yellow solid was collected by filtration and dried properly to give **L** 85mg (74.5%). ^{1}H NMR (500 MHz, CD_3CN, 25 °C, TMS) δ (ppm): 8.17-8.14 (m, 2H; ArH), 7.93 – 7.87 (m, 8H; ArH), 7.72-7.68 (m, 14H; ArH), 7.53– 7.49 (m, 12H; ArH), 3.97 (d, J = 15.5Hz, 4H; Ar -CH_2P). ^{13}C NMR (200 MHz, CD_3CN, 25 °C, TMS) δ (ppm): 26.72 (d, Ar -CH_2P), 115.58, 116.587, 126.944, 130.350, 130.452, 130.837, 134.120, 134.2, 134.973, 135.921 (Ar- and P-Ar). IR (KBr) ν_{max}/cm^{-1}: 3336, 1679, 1589, 1440, 1330, 1295, 1110, 837, 745, 689, 558, 513, ESI-MS (m/z): 757.59 ((M^+ - $2PF_6^-$), 63%), 903 ((M^+ - PF_6^-), 40%). Elemental analysis: $C_{52}H_{40}F_{12}O_2P_4$: calculated C (59.55), H (3.84); found C (60.12), H (3.53).

^{1}H NMR spectra of L
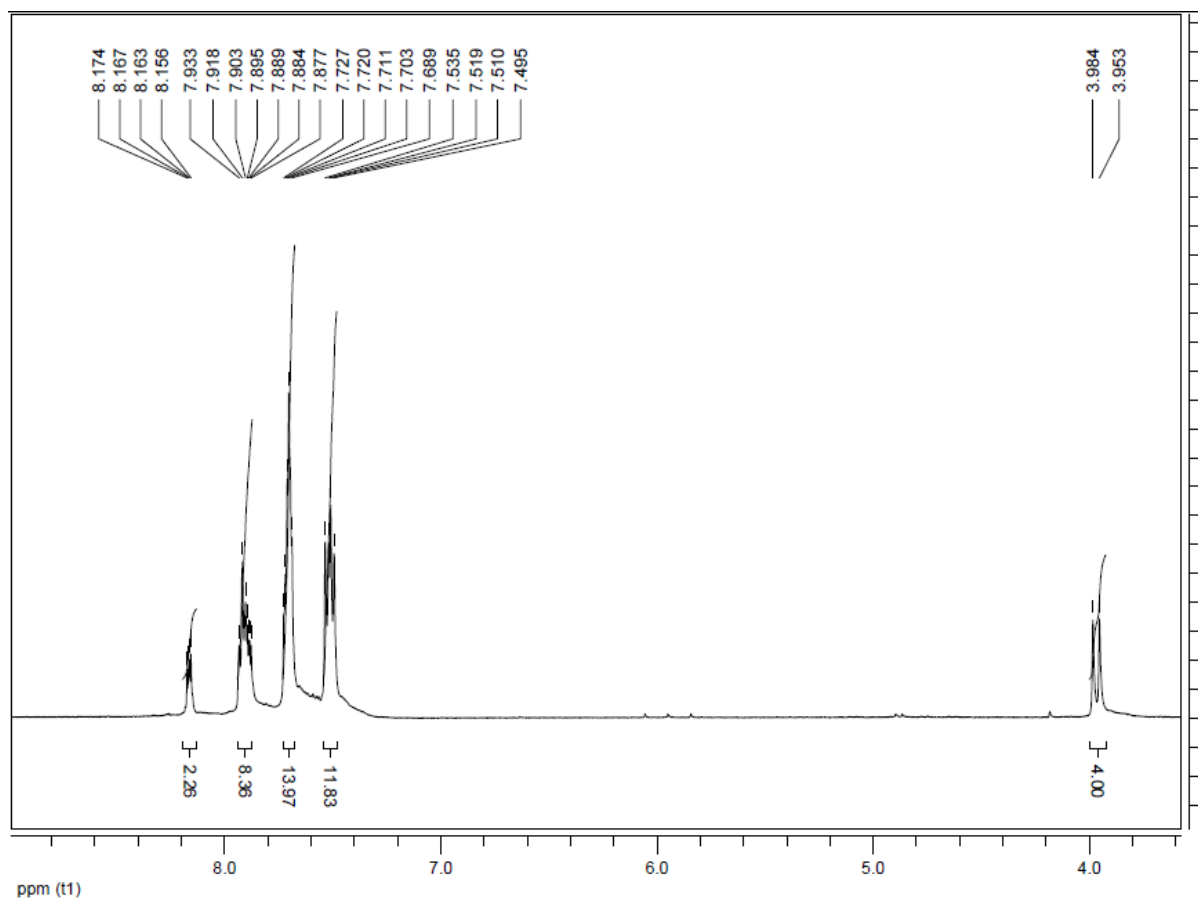
SI Figure 1:^{1}H NMR spectra of **L**

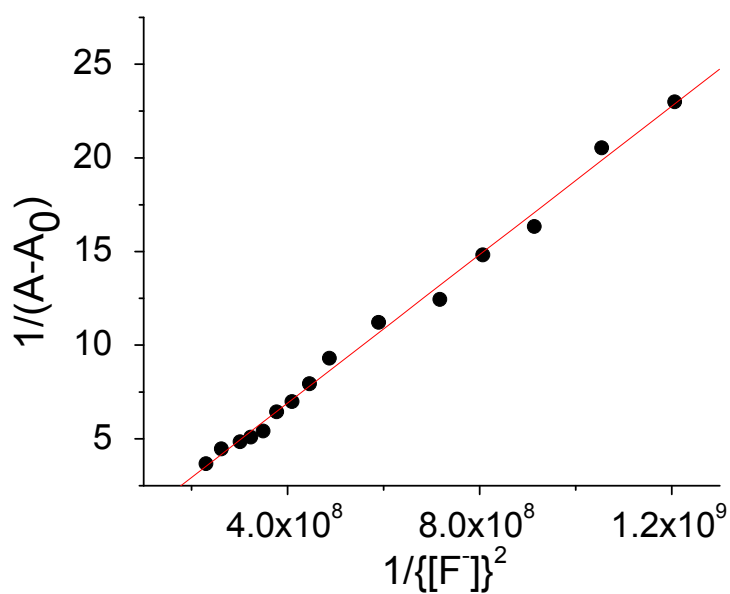## ^{13}C NMR spectra of L
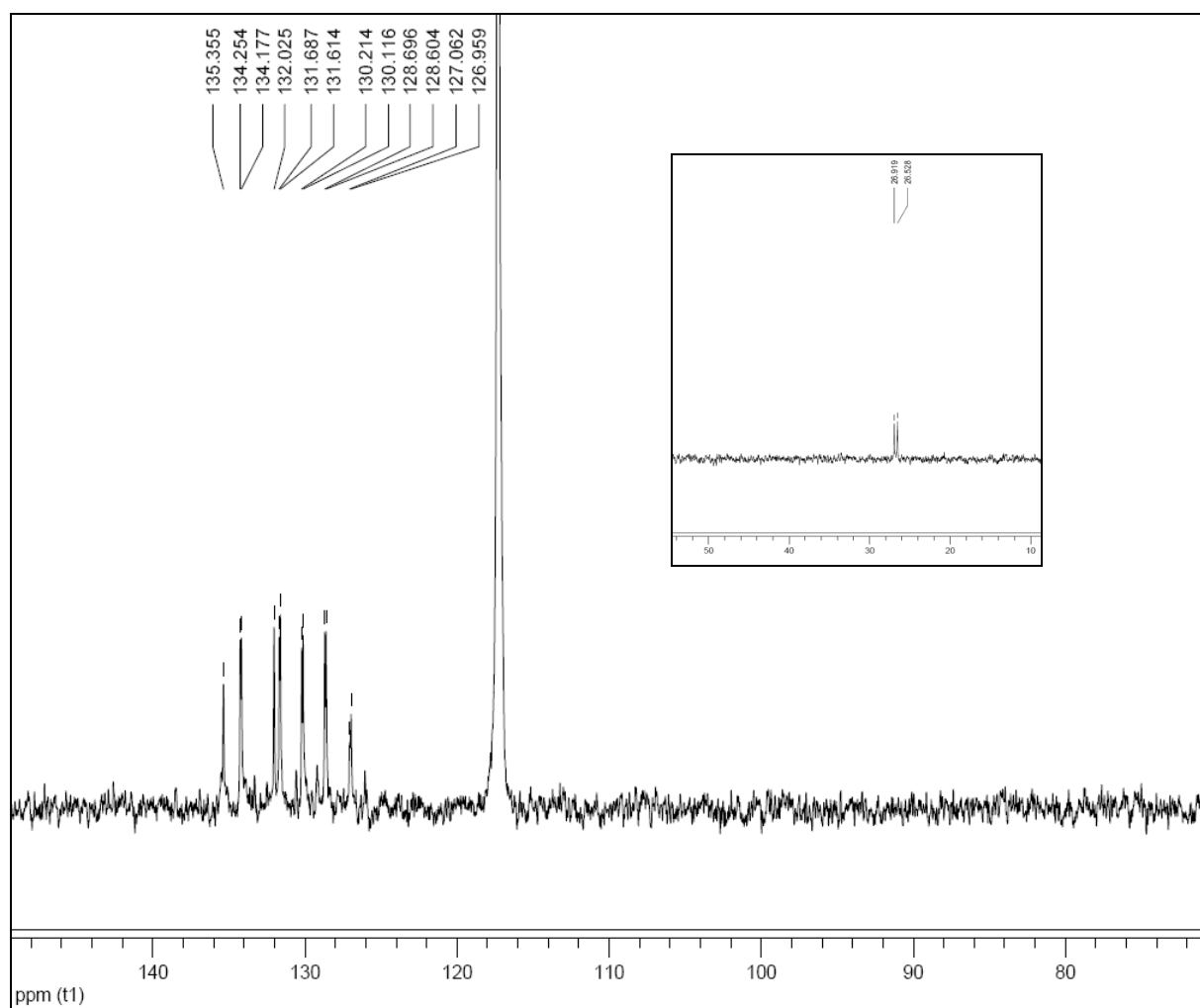
SI Figure 2: ^{13}C NMR spectra of **L**

UV- visible Titration of L with Fluoride
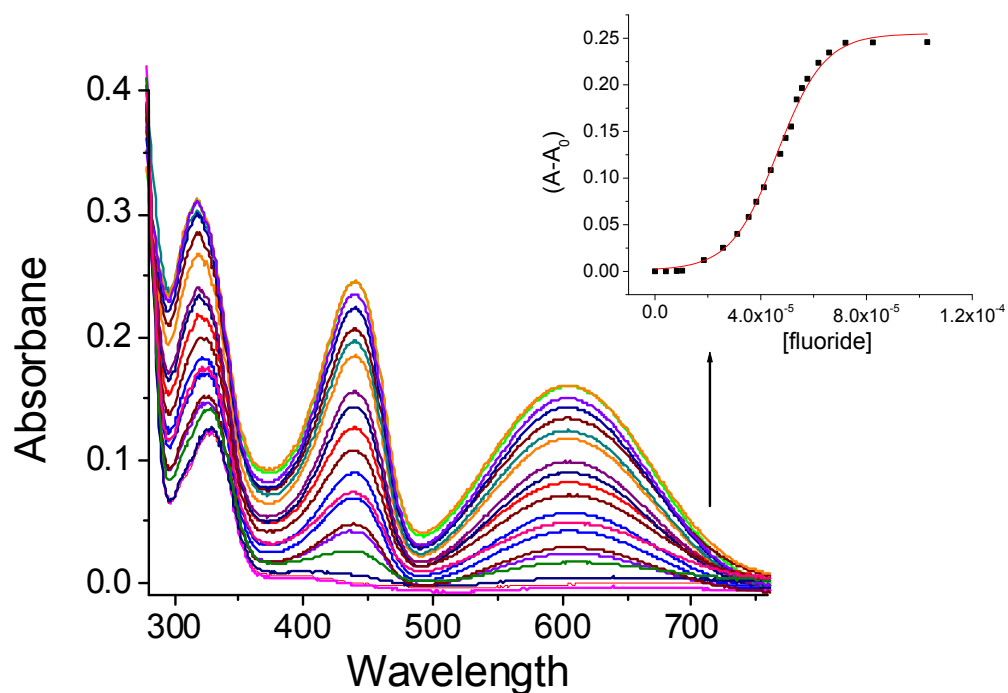
SI Figure 3: Absorption spectra of **L** (2.12 x10^{-5} M) in presence of varying concentration of Fluoride [0 – 8.24 x 10^{-5} M] in acetonitrile medium. Inset: corresponding titration plot of **L** at 440 nm (A-A_0) as a function of [F$^-$].

Benesi-Hildebrand plot of L with Fluoride

SI Figure 4: Benesi-Hildebrand plot of **L** with F$^-$ ion when monitoring absorbance changes at 440 nm shows the 1:2 stochiometry

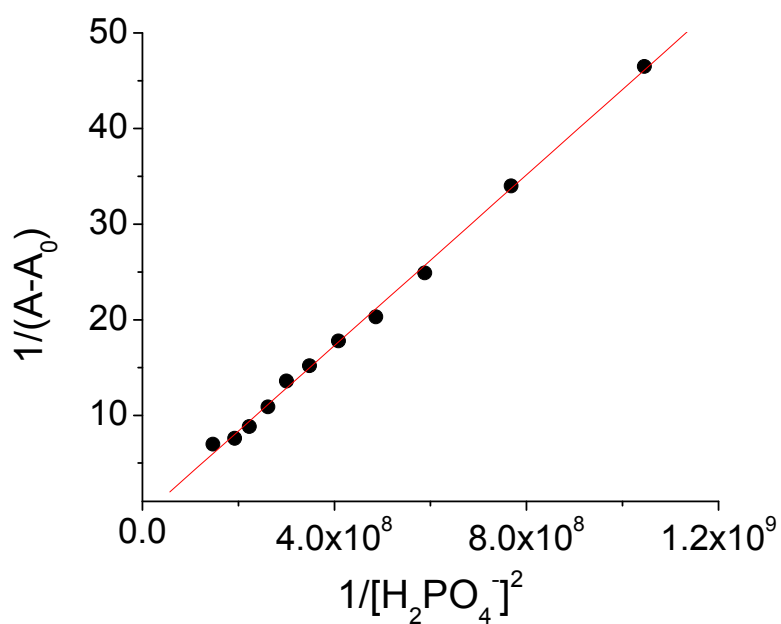**UV- visible Titration of L with di hydrogen phosphate**
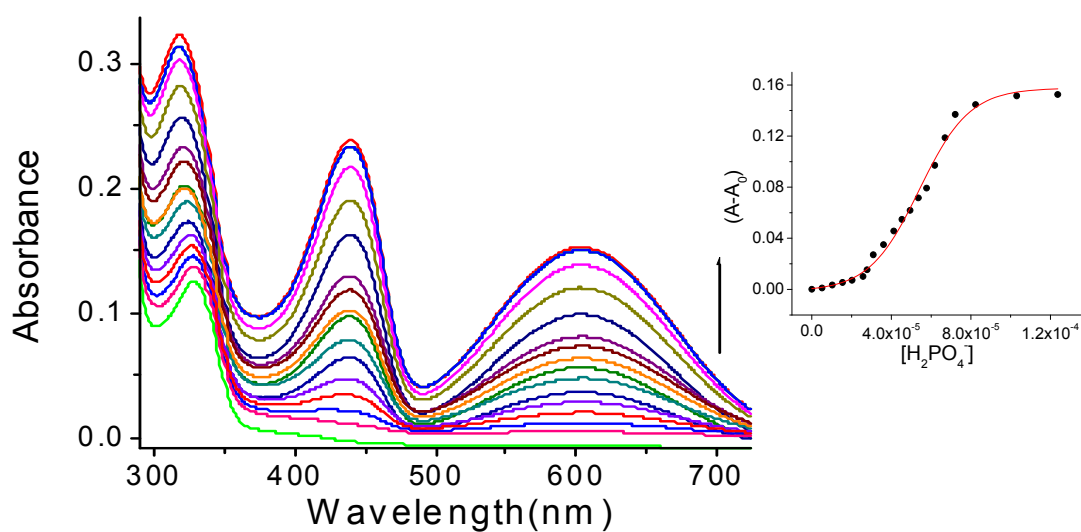
SI Figure 5: Absorption spectra of **L** (2.12 x10^{-5} M) in presence of varying concentration of $H_2PO_4^-$ [0 – 1.23 x 10^{-4} M] in acetonitrile medium. Inset: corresponding titration plot of **L** at 602 nm (A-A_0) as a function of [$H_2PO_4^-$]

Benesi-Hildebrand plot of L with di hydrogen phosphate

SI Figure 6: Benesi-Hildebrand plot of **L** with $H_2PO_4^-$ ion when monitoring absorbance changes at 602 nm show the 1:2 stochiometry
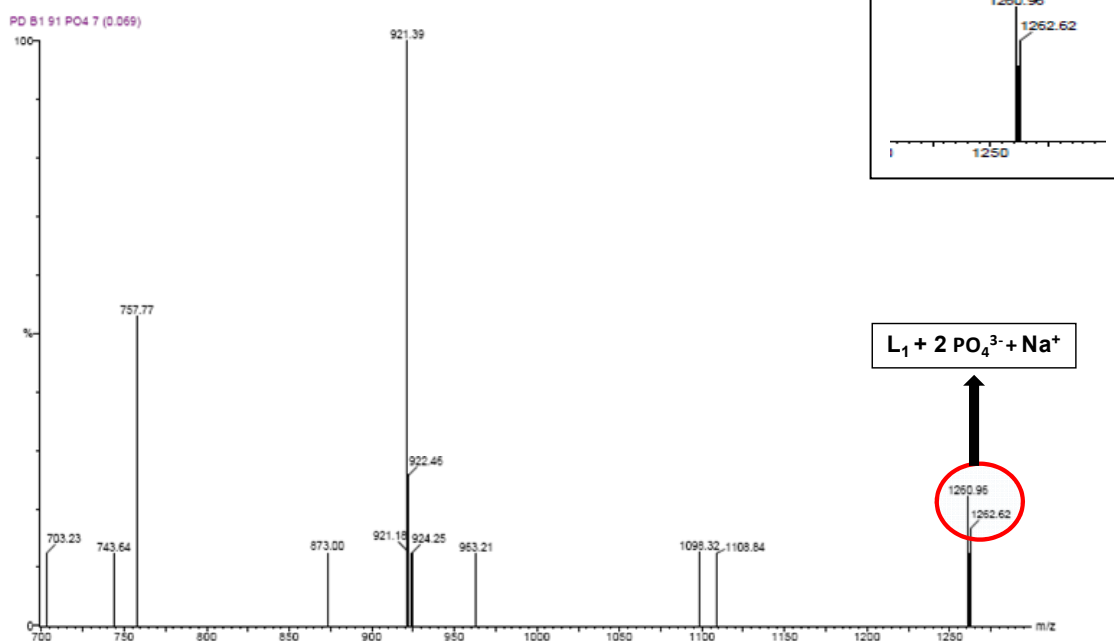
Mass spectra of (2:1) complex of Fluoride with L
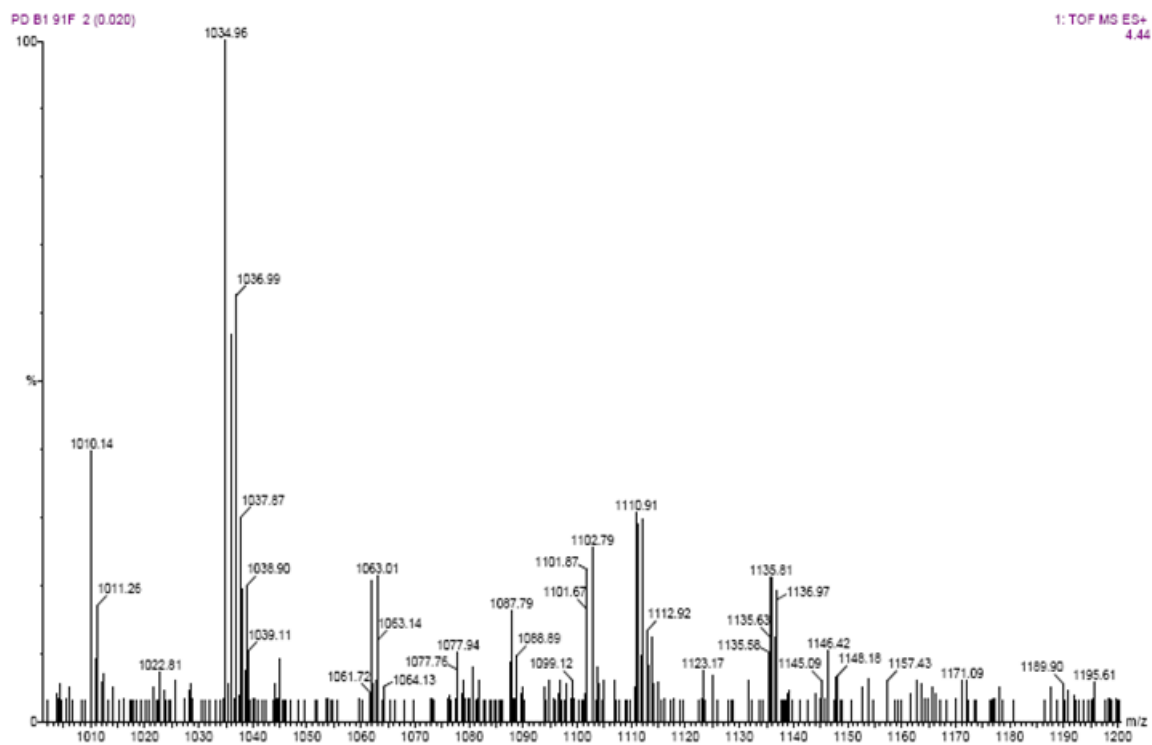
SI Figure 7: ESI-mass spectra of **L** in presence of 5 mole equivalent of added F⁻.

Mass spectra of (2:1) complex of $H_2PO_4^-$ with L

SI Figure 8: ESI-mass spectra of (1:2) complex of **L** & $H_2PO_4^-$

Mass spectra of extracted complex $L.2F^-$ $(H_2O)_2$ in CH_2Cl_2 layer.

$$L_1 - PF_6^- + 2\ F^- + 2\ H_2O + Na^+$$
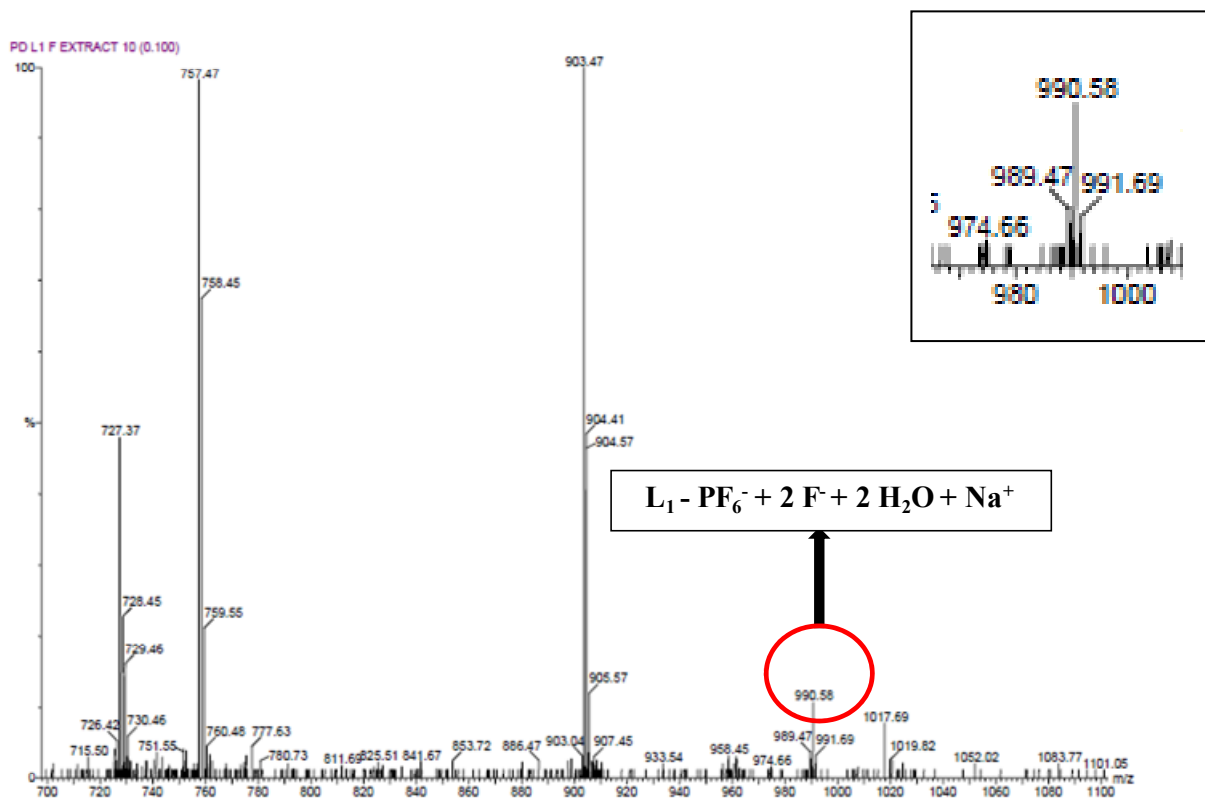
SI Figure 9: ESI-mass spectra complex of **L.2F⁻ (H₂O)₂** layer, which was extracted from aqueous solution of NaF.

^{1}H NMR of L with differnt anions at room temperature
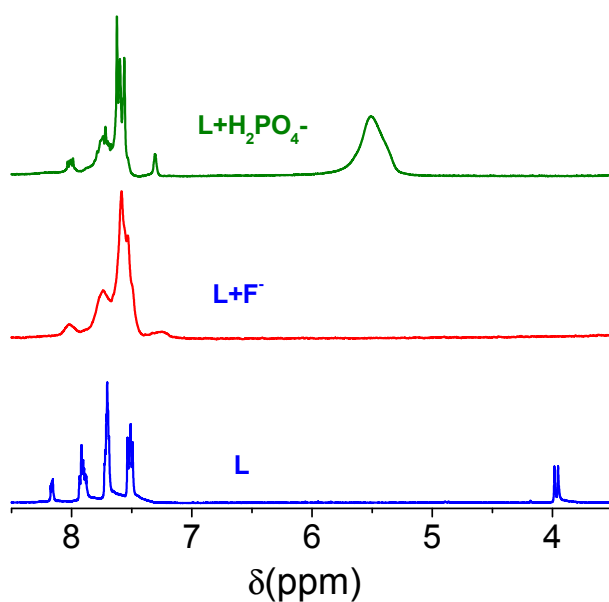
SI Figure 10: ^{1}H NMR spectra of compound **L** upon the addition of F$^-$, H$_2$PO$_4^-$ (50 mole equivalent) in CD$_3$CN at room temperature.
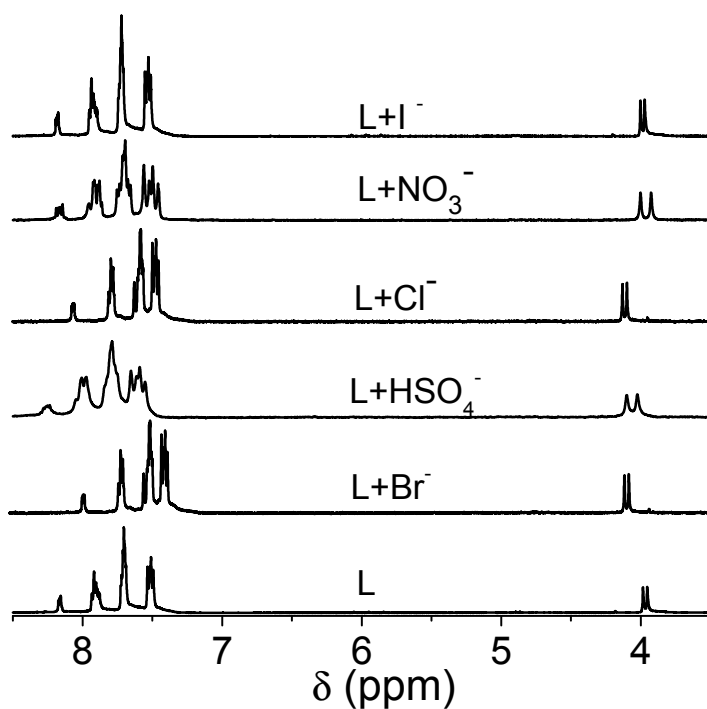
SI Figure 11: ^{1}H NMR spectra of compound **L** upon the addition of other different anions (50 mole equivalent) in CD$_3$CN at room temperature.

^{1}H NMR of L with excess (100 mole eq) of fluoride ion at room temperature
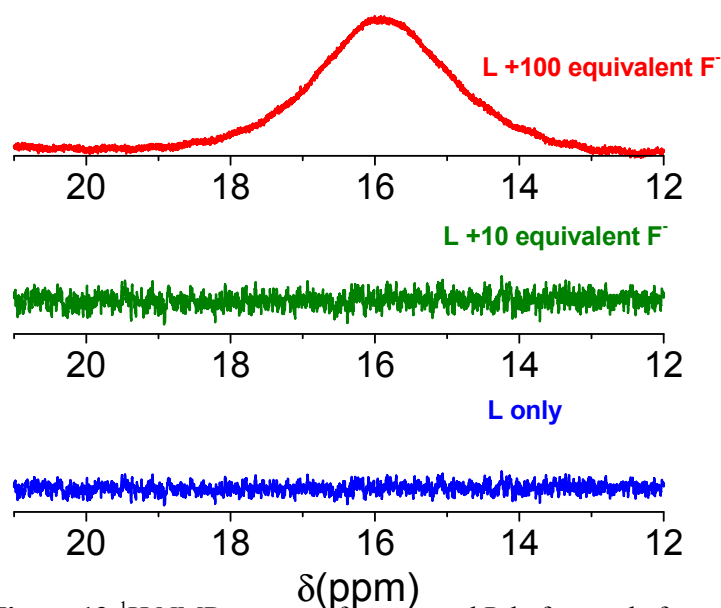
SI Figure 13: ^{1}H NMR spectra of compound **L** before and after addition of 100eq F$^-$ at room temperature in CD$_3$CN.

^{31}P NMR of L with presence of different anions
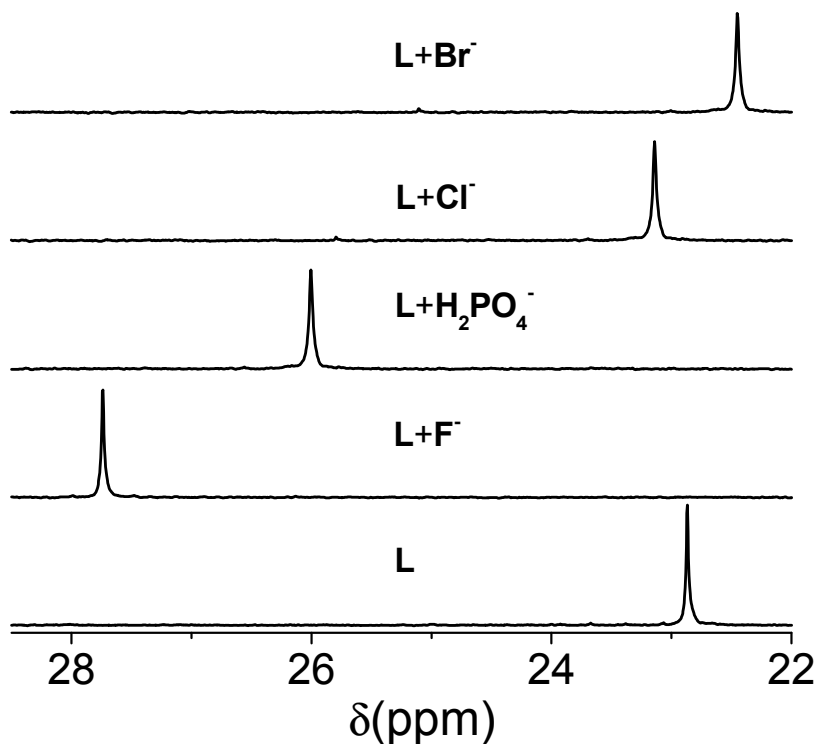
SI Figure 14: ^{31}P NMR spectra of compound **L** before and after addition of F$^-$, H$_2$PO$_4^-$ (5eq)and other Cl$^-$, Br$^-$ (30eq) in CD$_3$CN at room temperature.

14
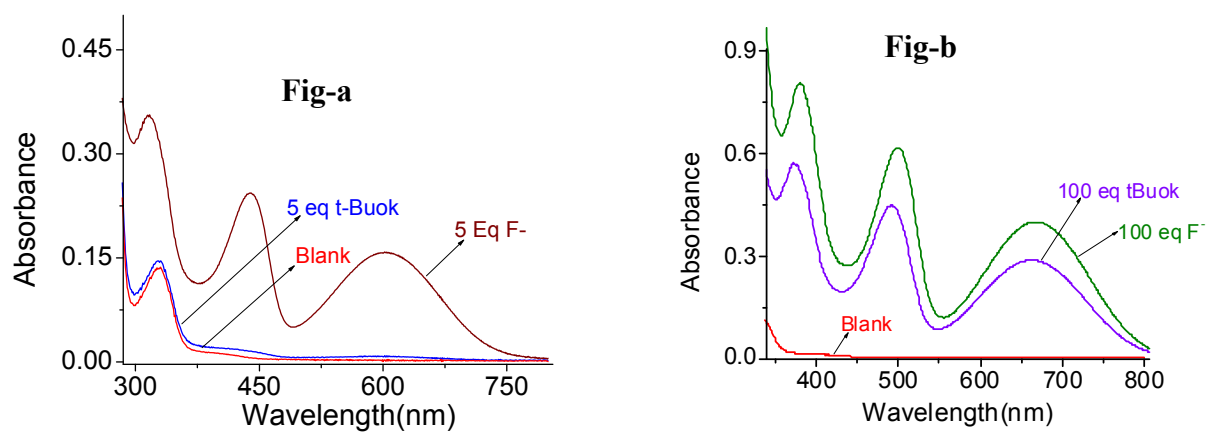
SI Figure 15: UV absorption change of **L** (2.12 x10^{-5} M) with (a) 5eq. F- and 5 eq. t-BuOK, (b) 100 eq. F- and 100 eq. t-BuOK in acetonitrile.

Computational methods

All geometries were fully optimized with Generalized gradient approximation (GGA) using BLYP functional integrated in density functional program DMol3 (version 4.1.2) of Accelrys Inc. The physical wave functions are expanded in terms of numerical basis sets. We used a DNP double numerical polarized basis set which is comparable to the 6-31G** basis set. All calculations were performed in gas phase.

$E_B = -328.6$ kcal/mol $E_B = -215.9$ kcal/mol

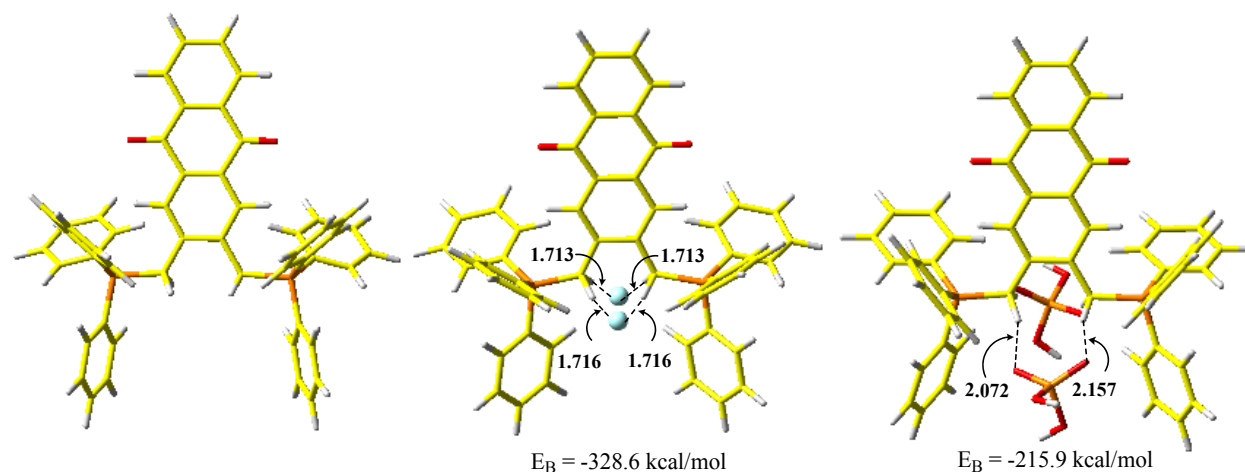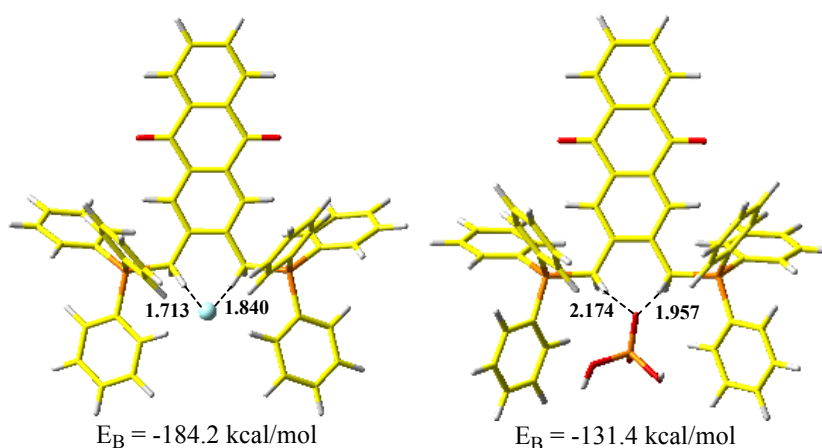**SI Figure 16.** GGA/BLYP/DNP optimized geometries of **L**, L.2F$^-$ and L.2H$_2$PO$_4^-$, and important distances (Å) and binding energies of L.2F$^-$ and L.2H$_2$PO$_4^-$ complexes. (yellow = carbon; red = oxygen; cyan = fluoride; orange = phosphorus; white = hydrogen).

$E_B = -184.2$ kcal/mol $E_B = -131.4$ kcal/mol

SI Figure 17. GGA/BLYP/DNP optimized geometries of **L**, L.F$^-$ and L.H$_2$PO$_4^-$, and important distances (Å) and binding energies of L.F$^-$ and L.H$_2$PO$_4^-$ complexes. (yellow = carbon; red = oxygen; cyan = fluoride; orange = phosphorus; white = hydrogen).

Extraction procedure:

General procedure: At first 15ml of aqueous solution of NaF having varying but known strength was taken in a 60 ml separating funnel. To this 15 ml of 1.0×10^{-4} M CH_2Cl_2 solution of **L** was added. Then it was extracted and the nonaqeous layer becomes greenish blue. Then the nonaqeous layer was collected and diluted 5 times; 1 ml of this extracted non-aqueous layer (i.e. CH_2Cl_2 layer) was diluted with another 4 ml of fresh CH_2Cl_2. After that the electronic spectra was recorded and the absorbance at 440nm was monitor to achieve the standard plot. For unknown sample analysis, we have diluted these samples as mentioned below.

Sambar lake : diluted 3 times, **Bhavnagar Sea Water**: dilued 5 times, **Okha sea water:** diluted 5 times So the value obtained from the standard plot was multiplied by the proper dilution factor to obtain the actual fluoride ion concentration of the analysed sample

Measurement of Extraction efficiency of L:

Known concentration of TBAF dissolved in CH_2Cl_2 solution was treated with CH_2Cl_2 (15 ml) solution of **L** to record the electronic spectra, then identical concentration of the aqueous solution of NaF was extracted several times (three times) with the CH_2Cl_2 solution of **L**. All non-aqueous layer were collected together, final volume was adjusted to 15 ml and after that the electronic spectra of the nonaqeous layer was recorded. Absorbance at 440 nm was compared with the previous one to get the extraction efficiency, which was found to be 99.3%.

Experiment for Phosphate interference:

Taken from "*Water, Water Everywhere***. HACH Company. Second Edition. 1991".**

Phosphates enter waterways from human and animal waste, phosphorus rich bedrock, laundry, cleaning, industrial effluents, and fertilizer runoff. These phosphates become detrimental when they over fertilize aquatic plants and cause stepped up eutrophication.

Phosphate is an essential nutrient for the proper growth of aquatic life (plant and animal). However, too much phosphate in the water has an adverse influence on the aquatic life and turns toxic and cause animal death. The optimum concentration for sea water between 0.05 to 0.20 mg/l (ppm) phosphate and beyond this, this is toxic to aquatic life.

Our Experiment:

We have used a 0.25 ppm of NaH_2PO_4 (pH 7.2 with 0.1 mM HEPES buffer medium) was used for extraction experiment using 15 ml 1.0 x 10^{-4}M of the reagent **L**. Neither any detectable colour in the nonaqueous layer (CH_2Cl_2), nor any measurable absorbance at 440 or 605 nm was obtained (Figure SI 17). This nullifies the possibility of phosphate interference in the measured fluoride ion concentration extracted in the nonaqueous layer.


SI Figure 18: Photograph for 0. 25ppm NaH_2PO_4 extraction by CH_2Cl_2 solution of **L**.

Interference Study during the extraction of fluoride in presence dihydrogen phosphate
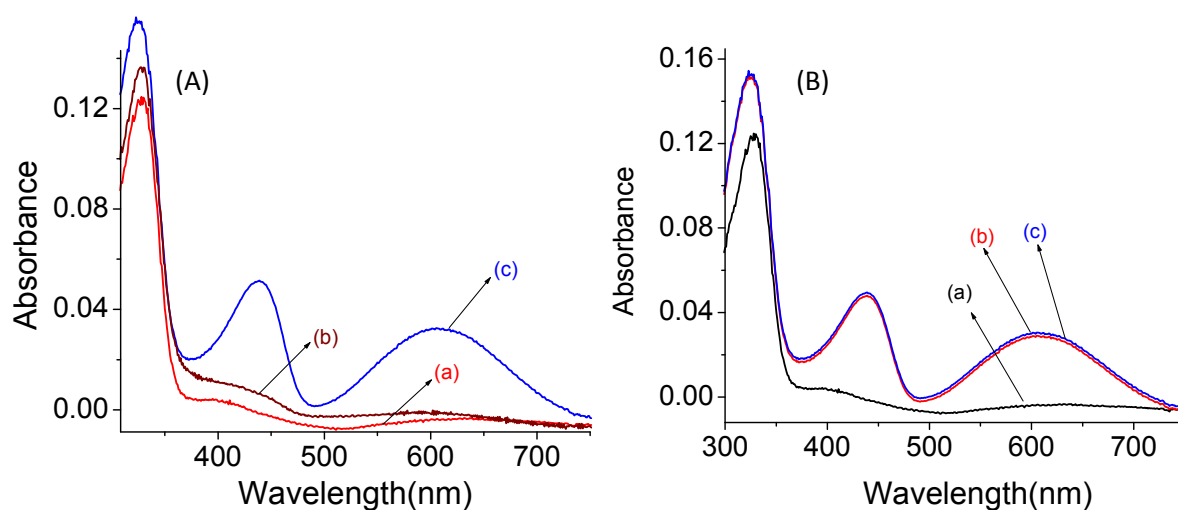

SI Figure 19: (A) (a) absorbance spectra of organic layer of **L** before extraction, (b) absorbance spectra of organic layer after extraction of aqueous solution of 2 ppm $H_2PO_4^-$, (c) absorbance spectra of organic layer after extraction of aqueous solution of 0.1 ppm F^-; (B) (a) absorbance spectra of organic layer of L before extraction, (b) absorbance spectra of organic layer after extraction of aqueous solution having a mixtutre of 0.1 ppm F^- and 20 equivalent of $H_2PO_4^-$, (c) absorbance spectra of organic layer after extraction of aqueous solution having of 0.1 ppm F^- only.

**Evaluation of the binding constant of L towards F⁻ from the extraction process**:
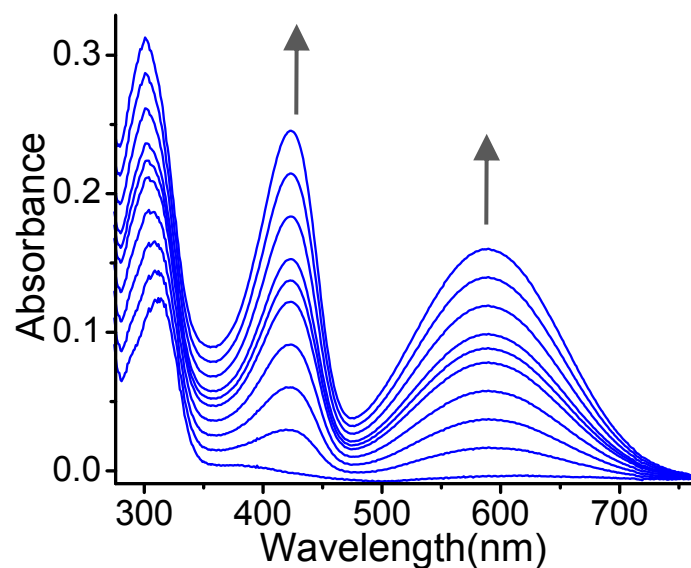
SI Figure 20: Absorption spectra of **L** (2.02×10^{-5} M) following solvent extraction process with varying concentration of NaF [$0 – 8.00 \times 10^{-5}$ M] in aqueous solution of neutral pH. Calculated binding constant for the formation of **L.2F⁻** was found to be $(1.7 \pm 0.15) \times 10^6 \text{M}^{-2}$, which is slightly lower than the value that was evaluated in pure acetonitrile medium. Higher salvation of F⁻ in aqueous solution could have accounted for this.

**^{1}H NMR of L with varying concentration of TBAF at -20°C**
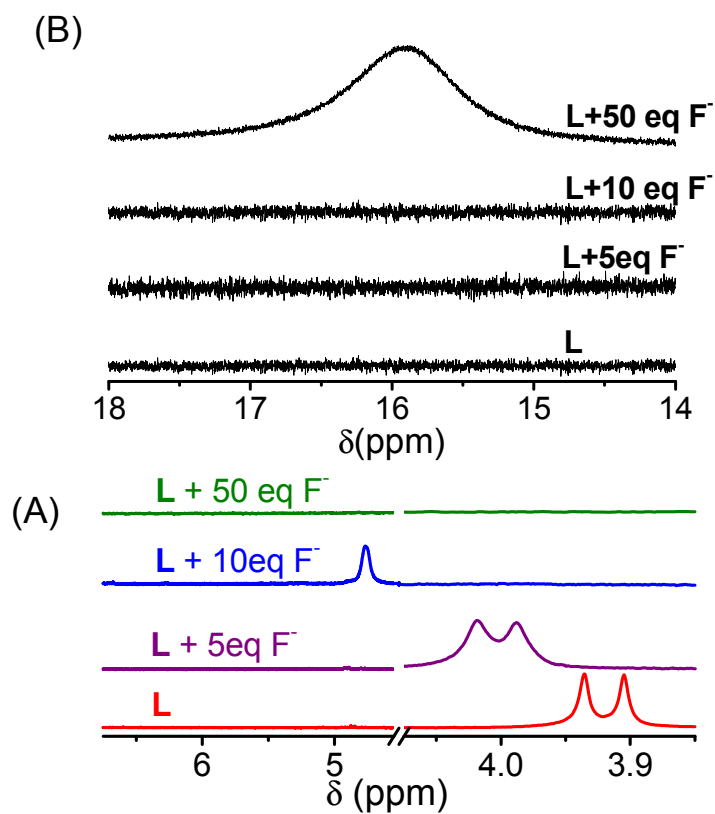
SI Figure 21: ^{1}H NMR spectra of compound **L** (A) upon the addition of varying concentration of F$^-$ in CD$_3$CN at -20°C; (B) Partial ^{1}H NMR spectra that reveals the generation of HF$_2^-$ on deprotonation of L in presence of excess of TBAF (50 mole equivalent) in CD$_3$CN medium at -20°C. Deprotonation of L or the generation of HF$_2^-$ was not evident with 10 mole equivalent of TBAF at -20 °C.

Uv-vis spectral titration of the extracted dichloromethane layer containing fluoride bound L at different pH from the aqueous solution containing a certain [F⁻]:
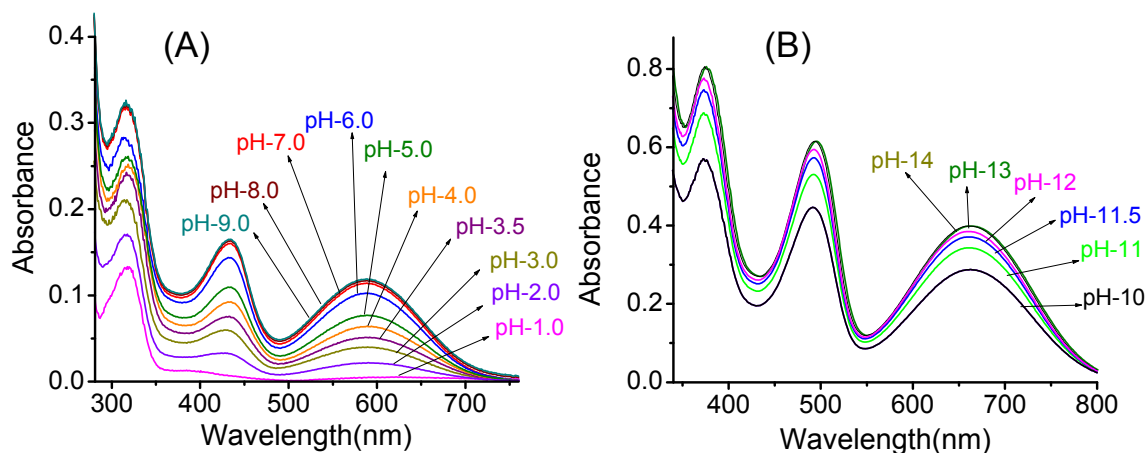
SI Figure 22: (A) and (B) are the Uv-vis spectra of the extracted fluoride bound solution of L (2.05×10^{-5}M) in dichloromethane at different pH from the aqueous solution of constant [NaF] (6.25×10^{-5}M).
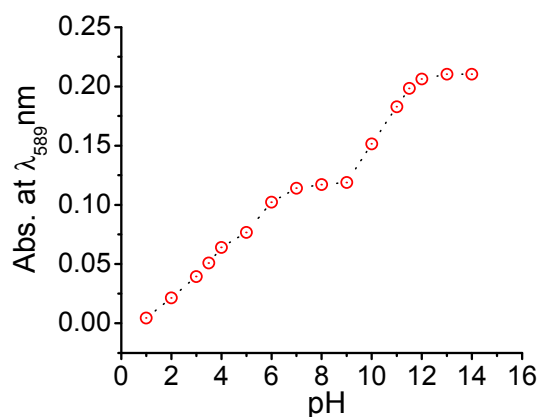
SI Figure 23: A plot of absorbance of the organic layer (CH_2Cl_2) after extraction from aqueous solution of 6.25×10^{-5} M NaF at 589 nm and varying pH of the aqueous solution.

At pH beyond 10 for the aqueous solution of NaF (6.25×10^{-5}M), a distinct change in spectral pattern and the associated shift in the λ_{max} is evident (λ_{max} shifts from 589 nm (pH range of 3.5-9) to 660 nm at pH beyond 10) , which perhaps signifies a different chemical processes involved at pH beyond 10. Extent of $L.2F_2^-$ formation was not significant at pH < 3.5.